

# Semi-Supervised Automated Layer Identification of X-ray Tomography Imaged PCBs

Ulbert J. Botero, Fatemeh Ganji, Navid Asadizanjani, Damon L. Woodard, Domenic Forte  
(jbot2016, fganji)@ufl.edu, (nasadi, dwoodard, dforte)@ece.ufl.edu

**Abstract**—Reverse engineering (RE) for printed circuit boards (PCB) can be achieved through X-ray Computed Tomography (CT) in a non-destructively yet predominantly manual process. For practical RE to be possible in applications such as obsolescence replacement and hardware assurance, it is important that this process be as automated and fast as possible. This paper introduces a framework to identify which slices of an X-ray CT 3-D PCB stack belong to what layer on a physical PCB in an automated and generalizable fashion for any X-rayed PCB. To the best of our knowledge, this is the first method for identifying the correspondence between an X-ray CT slice and layers of a PCB using reference design information, demonstrated on a 6 layered PCB. First, a spatial pyramid bag-of-visual-words technique is leveraged to enable a semi-supervised approach where the user has either digital or X-ray layout information available for heterogeneous image comparison between X-ray CT image slices. Second, a weighting scheme based on entropy of an image region is proposed. Our results show near perfect quantitative and qualitative layer identification. The completion of this step facilitates improved performance in later RE stages, such as feature extraction or analysis of an X-rayed PCB.

**Keywords**—printed circuit board; reverse engineering; machine learning; clustering; computer vision; pattern recognition; X-ray computed tomography.

## I. INTRODUCTION

The current state-of-the-art for reverse engineering (RE) of printed circuit boards (PCBs) is to use an X-ray Computed Tomography (CT) system to non-destructively reconstruct the PCB as a 3-D point cluster which can be analyzed to recover the board [1]. However, this technique introduces new challenges such as its reliance on subject matter experts to complete the RE process with this data. Even when image processing and computer vision algorithms are employed, there is still substantial manual effort needed in order to successfully RE the netlist on a sample by sample basis. Therefore, to address the shortcomings of the current state-of-the-art, these methods need to be automated. Automation of the RE process can be broken down into 5 major areas: image acquisition, image pre-processing, feature extraction, feature analysis, and evaluation [2].

This paper addresses a challenge seen at the pre-processing stage of the pipeline for PCB RE, namely automated layer identification. The unique aspect of this task is the necessity to use as little manual intervention as possible. Yet the great challenge remaining is that how much a priori information is available to the user conducting RE. If the user possesses “reference data”, or previous design info, it can be used to guide the identification process since the desired outcome is known. Perhaps the user does have access to the information regarding the design of the layout layers to guide the identification process, but in a digitally generated 8-bit image format.

In this case, identifying which X-ray CT slices of the 3-D volumetric PCB stack correspond to what layer in the physical PCB may prove difficult due to reference data being from a different imaging modality. This paper, for the first time to the best of our knowledge, addresses this heterogeneous image classification challenge for a generalizable, fully automated, and semi-supervised PCB layer identification process.

Specifically, the Spatial Pyramid Bag of Visual Words (SP-BoVW) technique is utilized for heterogeneous image comparison. More concretely, our approach compares PCB layer images taken either from a CAD software-generated layout or X-ray CT images, previously made from the PCB. In this regard, images of a layer are related to the X-ray CT imaged slices in a 3-D PCB stack. Furthermore, we propose adding an entropy-based weighting to the SP-BoVW to improve the performance of our semi-supervised layer identification. By conducting experiments on a real-world 6-layer PCB, the effectiveness of our method is demonstrated and elaborated upon in this paper. For this purpose, we have designed our PCB in house, referred to as RASC. . The contributions of this paper are summarized as follows: A framework for fully automated semi-supervised layer identification for X-ray CT imaged PCB slices, improved classification performance based on Entropy Weighting for Spatial Pyramid Bag of Visual Words, and heterogeneous image comparison/classification.

The remainder of the paper is organized as follows. Section II discusses our methodology in depth, whereas Section III provides a qualitative and quantitative analysis of the results. Lastly, Section IV concludes the paper.

## II. SEMI-SUPERVISED LAYER IDENTIFICATION METHODOLOGY

During the X-ray CT process for a PCB, the 3-D reconstruction of the sample is a stack of 2-D images referred to as slices. Acquiring the data in this fashion provides a reconstruction with the highest fidelity. However, relating the X-ray penetration and produced number of slices to a discrete depth in the physical PCB in order to identify the layers is no longer trivial. In order to effectively RE a PCB and provide full assurance, it is important that this information can be recovered under a number of use case scenarios, namely possessing a separately imaged reference layer of the layout via X-ray CT or its respective digital image extracted from a PCB manufacturer’s software. Nevertheless, there is a lack of information as to relate slices and their respective layers.

Furthermore, identification via simple pixel intensity based approaches, e.g., correlation analysis or Structural Similarity Index (SSIM) [3], are insufficient for the digital semi-

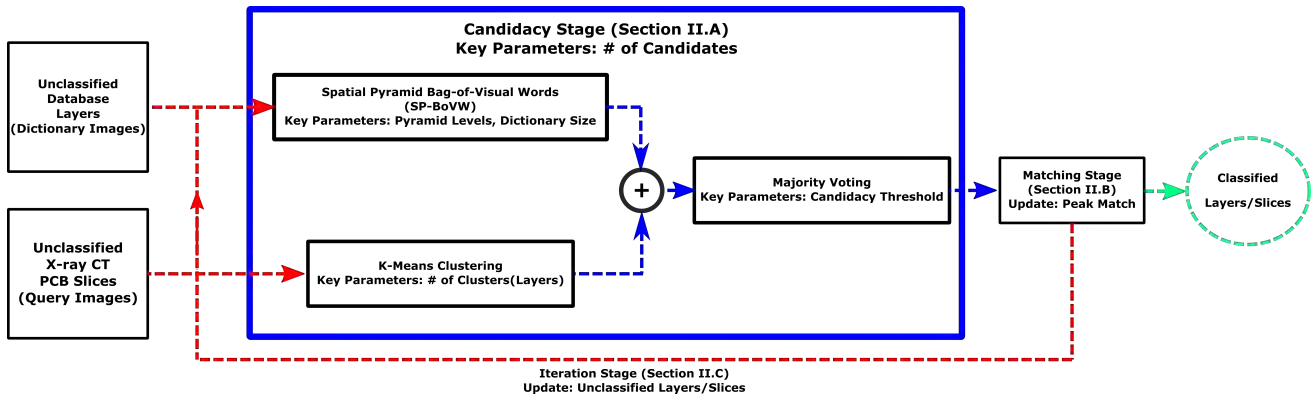


Fig. 1: Semi-Supervised Iterative Layer Identification Block Diagram

supervised case. This is due to the drastic difference in the textures of the X-ray images and the uniform texture seen across all the digital layer CAD images for the PCB. To highlight this, we perform slice-to-layer classification using a relatively naïve approach based on similarities between a slice and a layer in the database. The naïve approach shows the invalidity of the assumption that for any layer in a PCB stack, the number of slices fused together to form the layer image ( $n$ ) is the total number of slices divided by the number of known layers. Those slices are most similar to the layer in question according to pixel intensity based approaches. To demonstrate this, the similarity of each slice is compared to each layer in the database, with the highest match between a slice and layer assumed to be the correct correspondence. Due to the difference in texture, but similarities in the structure, SSIM is used for analyzing the similarities between an X-ray slice and a digital database layer. For X-ray slice to X-ray database layer comparison, the correlation is used due to being of the same modality. This approach recursively searches and adds a slice to a layer as long as it is in the highest  $n$  number of similarity scores for that layer. Nonetheless, the necessity for a more sophisticated approach is emphasized by classification accuracy of 36.31% and 70.70% for SSIM based classification using a digital reference and correlation based classification using an X-ray CT reference, respectively.<sup>1</sup>

In contrast, to overcome the limitations of the naïve approach, we propose an iterative slice to layer identification process, visually depicted in Figure 1, consisting of two main stages. First, there is a candidacy stage, utilizing clustering and bag-of-visual-words [4] to determine what layer the slices within each cluster corresponds to. This is followed by a matching stage where a layer image in the database is compared to a set of fused candidate images to select the optimal match. This framework validates the slices and layers in an iterative fashion until it reaches a point, where only one layer and one cluster of slices are not matched or all layers and slices are connected to one another.

#### A. Candidacy Stage

The candidacy stage begins by running an algorithm previously developed by us [5], where slice-to-layer classification

is achieved in an unsupervised manner with no reference data used or required. However, that result can be improved through adding reference information, as shown later in Section III. Specifically, our proposed framework first determines clusters of non-classified slices, and we subsequently use them as a starting point for each round of the iterative identification process. To determine these clusters for each round, especially the initial round, we leverage domain knowledge, namely X-ray CT imaged slices are stacked together sequentially and those adjacent slices have a high correlation with one another. Furthermore, for initial slice to layer identification, K-means clustering is an adequate algorithm since the number of layers is known beforehand. For this purpose, proper feature selection and the distance metric representing the correlation should be further adopted.

For the former, before conducting a correlation or clustering analysis, it is important to perform dimensionality reduction on the images, e.g., via Principal Component Analysis (PCA) [6], to project them to a much smaller dimensional space that still maintains their similarities and differences. In addition to nearby slices having a high correlation to one another, we leverage the fact that only slices directly near one another could ever belong to the same layer. Therefore, we apply an exponential windowing function to the correlation feature vectors used for clustering to drastically reduce the impact of slices being far away from slices that are under test for classification. The exponential window equation [7] is defined as  $w(X) = (\exp(j-i)/\tau)X_{i,j}$ , where  $X$  is the vector composed of the cross correlation of a slice with every other slices in the stack,  $i$  is the index of the current slice, and  $j$  represents the indices of all the other slices in the stack. The hyper-parameter  $\tau$  is a variable that can be adjusted to determine the width of the window. Empirically, it was determined that the optimal value of  $\tau$  is 6% of the total number of slices present in the stack. The resultant clusters of slices are now used as the starting points for each round of the semi-supervised iterative layer identification process.

With the cluster of slices serving as starting points, we then employ the Bag of Visual Words (BoVW) model [4] to identify the slices in each cluster that belong to their respective candidate layer. This process consists of, first, learning a visual feature dictionary for these images based on the extracted keypoints and descriptors of the Scale-Invariant Feature Transform

<sup>1</sup>The results for our proposed methodology is compared against the naïve approach later in Section III.

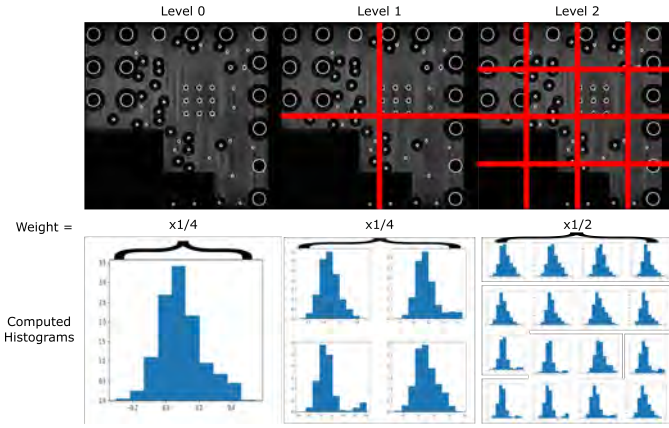


Fig. 2: High Level Example of Spatial Pyramid Bag of Visual Words Model

(SIFT) for the layer images [8], [9]. Afterward, the dictionary and vocabulary of the images are derived by clustering the descriptors via K-Means and computing a histogram of the frequencies for each feature to each cluster center, followed by re-weighting based upon the term frequency-inverse document frequency (tf-idf) weighting scheme [10]. Furthermore, since the images are quite similar to one another, with the discriminating features being the traces or copper plating and their locations, it is useful to take advantage of the Spatial Pyramid BoVW (SP-BoVW) model [11]. SP-BoVW divides an image into increasingly smaller blocks and repeats the dictionary and vocabulary learning process for each block of an image and concatenates them, giving more weight to the later level histograms calculated as the resolution gets finer the deeper into the pyramid one goes. Figure 2 provides a high level example of the process. The two main hyper-parameters for this stage in the framework are the depth of the spatial pyramid and the size of the dictionary. To maximize the amount of discriminative and spatial information we have chosen the spatial pyramid to have a level of 3 and the amount of clusters used to determine the dictionary to be 20% of the total amount of keypoints and descriptors extracted in a pyramid level.

Additionally, for this particular application we see that there are clearly regions of low information or zero information consistent throughout all layers in the PCB. Therefore, weighting all regions based on entropy will give less weight to the low information regions compared to those rich in information and thus improve the matching ability. The amount of information present in each image used for determining the weights are computed as the Shannon entropy of each sub image,

$$H(\text{Image}) = - \sum_{i=0}^{n-1} p_i \log_b(p_i), \quad (1)$$

where  $n$  is the number of gray levels in the image,  $p_i$  is the probability of a pixel having gray level  $i$ , and  $b$  is the base of the logarithm function. The weighting ( $w$ ) is done by determining the maximum and minimum entropy for the set of entropy values ( $\mathbb{H}$ ) computed on all the sub-images ( $\text{Image}_j$ ) at a particular pyramid level ( $l$ ), such that  $\mathbb{H} = \{H(\text{Image}_j), 0 \leq j < 4^l\}$ . Afterward, performing min-

max normalization on the entropy values for each subregion, the maximum weighting a sub region can be 1 and minimum is 0 (i.e., for very sparse regions). The kernel weighting is defined as

$$w(\text{Image}_j, l) = \frac{H(\text{Image}_j) - \min(\mathbb{H})}{\max(\mathbb{H}) - \min(\mathbb{H})} \quad (2)$$

$$k^L(X, Y) = \frac{1}{2^L} I^0 + \sum_{l=1}^L \frac{1}{2^{L-l+1}} w(\text{Image}_j, l) I^l, \quad (3)$$

where  $j$  is a sub-image at a particular pyramid level ( $l$ ),  $L$  represents the total amount of levels to be used in the pyramid, and  $I$  is the intersection of the histograms  $X$  and  $Y$  using the histogram intersection kernel [12]. The higher the output of this kernel, the more similar the two histograms, and thus images are based on their vocabularies.

The appropriate entropy and tf-idf weighted histograms of each level in the pyramid are concatenated and represent features of each layer in the database. The features of the slices in the PCB stack are computed in a similar fashion using the dictionary and weights determined during the creation of the dictionary for each level of the pyramid from the database. Now the information regarding what slices belong to which clusters is used to refine the clustering results. Specifically, we compute the histogram intersection match score of each slice in a cluster of the layers with respect to the layers in the database and compute the max score, being likely its best fit. Then, for the slices in the list we perform a majority voting, where the statistical mode of the slices in that clustered layer is chosen as the likely identified layer candidate in the database.

A candidacy threshold is determined by computing the average correlation of all layers in the database with one another and subtracting that from 1. This represents the average amount of unique information between all images in the database. If the percentage for the consensus layer decided per all the slices in a cluster is higher than the calculated threshold, we count the slices and layers as satisfying the candidacy criteria and pass them onto the matching stage.

### B. Matching Stage

The matching stage computes the matched points between the SIFT descriptors of the candidate image, consisting of the slices for that particular layer fused together, and respective database layer layout image. This process involves two steps described below.

1) *Digital Reference*: For digital database, where images are compared to X-ray slices, it is necessary to binarize the digital images of the layout layers in the database. After that, Contrast Limiting Adaptive Histogram Equalization (CLAHE) is performed on the X-ray layer image fused from slices in the respective cluster/layer prior to matching. Since CLAHE has been shown to improve SIFT point matching [13], these operations optimize the point matching between the two modalities regardless of image acquisition quality for X-ray or original layer color for the digital layer layouts.

2) *X-ray CT Reference*: X-ray to X-ray matching benefits from CLAHE for the same reasons mentioned above, but the binarization post-processing for the layers in the database is not necessary as both are imaged using the same modality.

### C. Iteration Stage

The entire candidacy and matching process is repeated until candidacy has been passed by a number of times predefined by the user. During this process, each time the number of matched SIFT descriptors is compared to the previous maximum, updated if necessary. According to our experimental results, passing the candidacy and matching process three times should be sufficient in our scenario. However, this threshold could be increased for higher confidence at the cost of increased computation time. As the quality of the fused image improves, so does the amount of matched SIFT points; therefore this serves as the final evaluation criteria for a matched layer identification. After finding a successful match, the corresponding slices and their respective layer are removed from the stack/database. The remaining slices and layers have yet to satisfy the identification criteria and thus, are left in the stack/database for more iterations.

Afterward, we recreate the dictionary and vocabulary of the images of the layout layers in the database, but now with only the unsatisfied layers in the database. This results in a reference vocab and the unsatisfied slices as the query vocab. Once the dictionary of vocab has been recreated for both the reference and query images, the candidacy and matching processes as well as the identification criteria are the same as previously mentioned. This process eventually converges to an end when all slices and layers have been satisfied or there remains only one group of slices and its respective layer being unsatisfied. In the event that during a single round multiple clusters satisfy candidacy for the same database layer, the cluster of slices that results in the highest amount of paired matching points is taken to be the correct identification and the remaining slices are put back into the group to be re-evaluated in the next iteration.

## III. RESULTS AND EVALUATION

### A. Experimental Setup

Our dataset experimented upon was a 6-layer PCB, referred to as RASC, with dimensions of 15mm by 15mm. This board was designed in house to provide access to ground truth data in the form of digital design software images and X-ray CT layer images. The X-ray CT image acquisition parameters for the dataset were a source voltage of 75kv, source current of  $573\mu\text{a}$ , pixel size of  $11.30\mu\text{m}$ , filter of 0.5mm Aluminum, exposure time equal to 38ms, and using a flat panel camera. The reconstruction parameters are a beam hardening coefficient of 43%, ring artifact of 18%, a gaussian smoothing kernel of sigma equal to 2, and a post alignment value of 7.7. After proper alignment, registration, and removal of all slices containing only air, the final size of the dataset resulted in a 3-D stack of  $1357 \times 1286 \times 157$  slices for the 6 layer board. Furthermore, these experiments were conducted on a non-populated version of the board.

### B. Quantitative Analysis

There are currently no established metrics to evaluate the different stages of the RE process or its quality. However, classification and clustering evaluation metrics can be leveraged by treating the slice to layer identification task as a

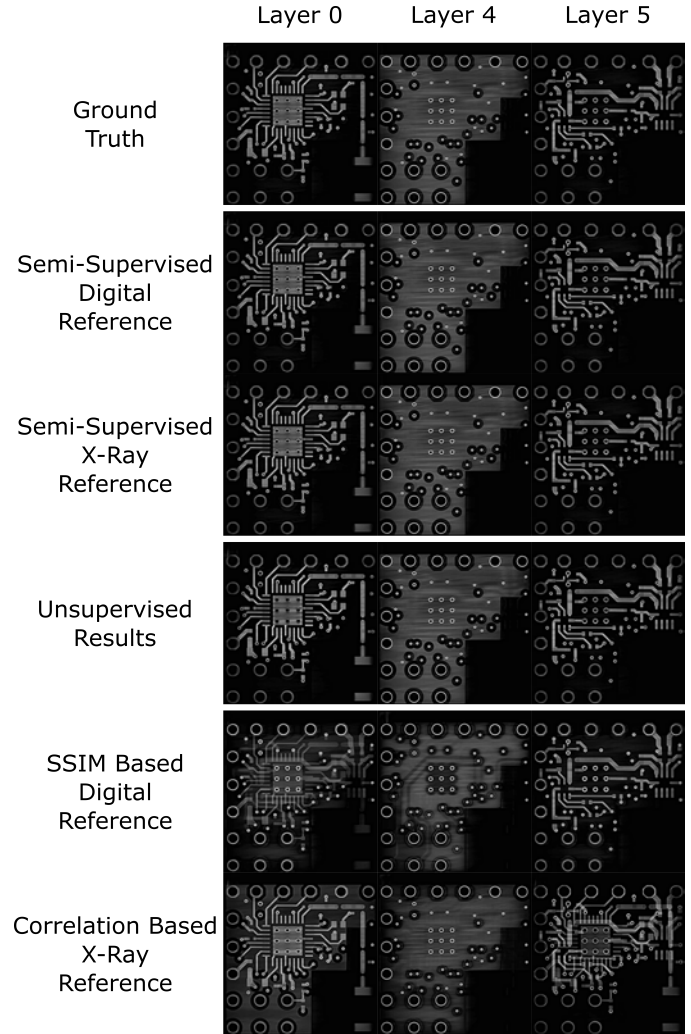


Fig. 3: Semi-Supervised Classification Results

classification and clustering problem, where each layer is a different class and cluster for their respective slices. For these metrics the ground truth for comparison are the labels of what slices belong to what specific layers after human evaluation and assignment. Appropriate metrics from a classification perspective are precision, recall, and the resulting F1-Score. These metrics provide an important understanding of false and true positive classifications so false positive classifications do not negatively affect the fusion of the image of a layer. If a false classification does occur, it could lead to the image containing false/aliased features from another layer or obscure important features that need to be extracted in later RE steps. From a clustering perspective, the appropriate measures are homogeneity and completeness. Using ground truth labels, these measures evaluate the effectiveness of semi-supervised approaches for each modality, where each cluster contains only slices of a single layer and all slices that belong to a particular layer are assigned to the same layer.

In Table I the aforementioned metrics are compared for the naïve approach mentioned in Section II, the unsupervised approach, and both iterative semi-supervised approaches (digital and X-ray CT layout) and the weighting schemes using

Method	Precision		Recall		F1-Score		Homogeneity		Completeness	
No Weighting	96.18%	96.18%	96.18%	96.18%	96.18%	96.18%	.922	.931	.921	.932
TF-IDF	97.2%	98.34%	97.2%	98.34%	97.2%	98.34%	.942	.968	.943	.967
Entropy	96.18%	97.07%	96.18%	97.07%	96.18%	97.07%	.922	.947	.921	.947
TF-IDF + Entropy	97.07%	97.64%	97.07%	97.64%	97.07%	97.64%	.940	.955	.940	.956
Unsupervised	90.51%		90.51%		90.51%		.828		.836	
SSIM Based Digital Reference	36.31%		36.31%		36.31%		.357		.354	
Correlation Based X-Ray Reference	70.70%		70.70%		70.70%		.547		.542	

TABLE I: Semi-supervised classification performance compared across approaches and weighting schemes.

Layer	SSIM - Digital Reference		Correlation - X-ray Reference		Unsupervised		Iterative S.S. - TF-IDF			
	SSIM	Correlation	SSIM	Correlation	SSIM	Correlation	SSIM	Correlation	SSIM	Correlation
0	.6487	.6541	.6713	.9305	.9053	.9871	1.0	1.0	1.0	1.0
1	.8268	.8752	.9026	.9525	.9907	.9985	.9991	.9949	.9998	.9991
2	.9211	.9671	.9377	.9928	.9916	.9984	.9951	.9958	.9994	.9992
3	.9469	.9866	.8473	.9537	.9913	.9967	.9936	1.0	.9980	1.0
4	.8341	.9246	.8923	.9603	.9923	.9993	.9957	1.0	.9994	1.0
5	.7182	.7979	.8127	.9497	.9733	.9993	1.0	1.0	1.0	1.0

TABLE II: Image quality assessment comparison across approaches and iterative semi-supervised (S.S.) with TF-IDF weighting.

tf-idf, entropy, entropy and tf-idf, as well as no weighting. These results are the average after running the algorithms 20 times. As expected, the earlier mentioned naïve approaches were by far the worst and the X-ray CT layout iterative semi-supervised approach outperforms all, including the digital. The superiority of the iterative semi-supervised approach using X-ray reference data is expected since the modality of the layout data and the slices is the same; hence, it should detect and match keypoints better than the algorithm using the digital layouts. However, the performance of the iterative semi-supervised identification with digital layout information is still satisfactory considering the incorrectly classified slices are likely fringe slices with minimal feature information. Therefore, their influence is felt when computing quantitative classification performance metrics, but overall has very little impact (see Figure 3). In contrast, reliance of the naïve approaches upon pixel intensity information with no location reference has resulted in several false classifications and aliasing of layers(see Figure 3).

Moreover, after taking all quantitative classification measures into account, it is important to recall that the main purpose of this stage in the RE process is to produce a high quality image that can be used for later stages. As a result, as long as the fused images are not drastically distorted, the result is satisfactory; however, for this analysis, it is important to measure the level of distortion quantitatively. To achieve this, we leverage Structural Similarity Index (SSIM) [3] and correlation. SSIM and correlation, which are metrics evaluating the pixel level distortion seen between a reference image and test image, bounded between 0 and 1.

Taking these metrics into account, Table II displays the average image quality assessment results after 20 trials for each layer of the RASC board. These results achieved through iterative semi-supervised layer identification for both digital and X-ray layer layout images using the top performing weighting in Table I, TF-IDF, as well as the naïve approaches and unsupervised method. For the computation of these metrics the images serving as the ground truth are the fused

images of each layer derived from human labeled whereas the “distorted” test images are the fused images of the different approaches.

Looking at the table, one can see the optimal performance occurs when the user has X-ray CT layout side-information available to guide the slice to layer identification process. However, the second best results are obtained for the semi-supervised approach with digital layout information. Again the naïve approaches perform the worst across due to the incorrectly classified slices, creating aliasing during the fusion of slices for the resultant layer images. The distortions seen for the iterative semi-supervised methods, mostly at the internal layers, could be from fringe slices for the power and ground plane. When being clustered incorrectly into the layers that also had copper plating, their effect is evident in terms of pixel-level quantitative quality assessment. Nevertheless, it is minimal qualitatively when viewing the output images, as shown in Figure 3.

#### IV. CONCLUSION

In conclusion, this paper leveraged the popular Spatial Pyramid Bag of Visual Words for heterogeneous image comparison between digital or X-ray CT PCB layer layout images and X-ray CT PCB slices to successfully achieve semi-supervised slice-to-layer identification. We also proposed the improvement of these techniques by introducing a weighting scheme that takes entropy of the sub-regions in the spatial pyramids into account. Now that this step in the automation process for PCB RE has been completed, we shall tackle the problem of feature identification (traces, vias, copper planes, etc) and vectorization in future work.

#### ACKNOWLEDGMENT

This material is based upon work supported by the National Science Foundation Graduate Research Fellowship under Grant No. DGE-1315138 and DGE-1842473.

## REFERENCES

- [1] N. Asadizanjani, M. Tehranipoor, and D. Forte, "PCB Reverse Engineering Using Nondestructive X-ray Tomography and Advanced Image Processing," *IEEE Transactions on Components, Packaging and Manufacturing Technology*, vol. 7, no. 2, pp. 292–299, 2017.
- [2] U. J. Botero, R. Wilson, H. Lu, T. Rahman, M. A. Mallaiyan, F. Ganji, N. Asadizanjani, M. M. Tehranipoor, D. L. Woodard, and D. Forte, "Hardware Trust and Assurance through Reverse Engineering: A Survey and Outlook from Image Analysis and Machine Learning Perspectives," Tech. Rep.
- [3] Z. Wang, E. P. Simoncelli, and A. C. Bovik, "Multi-scale structural similarity for image quality assessment," in *Conference Record of the Asilomar Conference on Signals, Systems and Computers*, vol. 2, 2003, pp. 1398–1402.
- [4] J. Sivic and A. Zisserman, "Video google: A text retrieval approach to object matching in videos," *Proceedings of the IEEE International Conference on Computer Vision*, vol. 2, pp. 1470–1477, 2003.
- [5] U. J. Botero, N. Asadizanjani, D. L. Woodard, and D. Forte, "A Framework for Automated Alignment and Layer Identification of X-Ray Tomography Imaged PCBs," in *GOMACTech*, San Francisco, 2020.
- [6] J. Shlens, "A Tutorial on Principal Component Analysis," 2014. [Online]. Available: <http://arxiv.org/abs/1404.1100>
- [7] J. O. Smith, *Spectral Audio Signal Processing*, 2011. [Online]. Available: <https://ccrma.stanford.edu/jos/sasp/> <http://books.w3k.org/>
- [8] D. G. Lowe, "Object Recognition from Local SIFT.pdf."
- [9] —, "Distinctive image features from scale-invariant keypoints," *International Journal of Computer Vision*, vol. 60, no. 2, pp. 91–110, 2004.
- [10] R. Grycuk, M. Gabryel, M. Korytkowski, and R. Scherer, "Content-Based Image Indexing by Data Clustering and Inverse Document Frequency," *Communications in Computer and Information Science*, vol. 424, pp. 374–383, 2014.
- [11] S. Lazebnik, C. Schmid, and J. Ponce, "Beyond bags of features: Spatial pyramid matching for recognizing natural scene categories," *Proceedings of the IEEE Computer Society Conference on Computer Vision and Pattern Recognition*, vol. 2, pp. 2169–2178, 2006.
- [12] A. Barla, F. Odone, and A. Verri, "Histogram intersection kernel for image classification," in *IEEE International Conference on Image Processing*, vol. 3, 2003, pp. 513–516.
- [13] R. D. P. Olvera, E. M. Zerón, J. C. P. Ortega, J. M. R. Arreguín, and E. G. Hurtado, "A Feature Extraction Using SIFT with a Preprocessing by Adding CLAHE Algorithm to Enhance Image Histograms," *Proceedings - 2014 IEEE International Conference on Mechatronics, Electronics, and Automotive Engineering, ICMEAE 2014*, pp. 20–25, 2015.